Journal of Hydrology 612 (2022) 128144

Contents lists available at ScienceDirect

Journal of Hydrology

journal homepage: www.elsevier.com/locate/jhydrol

Research papers

Throughfall drop sizes suggest canopy flowpaths vary by phenophase

Kazuki Nanko [a,*], Richard F. Keim [b], Sean A. Hudson [c,1], Delphis F. Levia [c,d]

[a] Department of Disaster Prevention, Meteorology and Hydrology, Forestry and Forest Products Research Institute, Ibaraki 305-8687, Japan
[b] School of Renewable Natural Resources, Louisiana State University, Baton Rouge, LA, USA
[c] Department of Geography & Spatial Sciences, University of Delaware, Newark, DE, USA
[d] Department of Plant & Soil Sciences, University of Delaware, Newark, DE, USA

ARTICLE INFO

This manuscript was handled by Marco Borga, Editor-in-Chief, with the assistance of Andres Iroume, Associate Editor

Keywords:
Canopy interception
Throughfall
Disdrometer
Residence time
Plant trait
Phenology

ABSTRACT

Water flowpaths caused by incident rainfall onto forest canopy surfaces have a notable effect on the water budgets and chemistry of wooded ecosystems. This study revealed varying canopy flowpaths and residence times at the intra-event scale and across the phenological transition from leafed to leafless states for a set of three American beech (*Fagus grandifolia* Ehrh.) trees in a multilayered canopy. Simultaneous measurements of raindrops and throughfall drops by fifteen laser disdrometers over five rain events were analyzed during the transition from leafed to leafless phenophases. Throughfall was partitioned into free throughfall, splash throughfall, and canopy drip with four drop size classes. Throughfall drop size distributions and volume of each throughfall type varied at both intra-event and inter-event scales. Smaller canopy drips, <5.5 mm in diameter, were initiated earlier in rain events, whereas more rainfall accumulation was necessary to generate larger canopy drips, >5.5 mm in diameter. Smaller canopy drips were more dominant in the leafed phenophase when some structurally-mediated woody surface drip points were more muted. These results suggested throughfall from foliar surfaces generated smaller-sized canopy drip with shorter residence time, whereas throughfall from structurally-mediated woody surface drip points generated larger-sized canopy drip with longer residence time. There was also an increase in both free throughfall and splash droplets from leafed to leafless states, consistent with increased canopy gaps and direct interaction with woody surfaces in the leafless state. Based on the results, a conceptualization of the genesis and development of leaf and branch flowpaths in canopies is proposed.

1. Introduction

Storage in, transit through, and release of precipitation from forest canopy surfaces has great consequences for water budgets and ecosystems, but the details of these processes remain poorly understood. Temporally varying water storage is a crucial factor controlling evaporation rates from wet canopies (Horton, 1919), but is difficult to measure directly or to constrain through indirect methods. The most common technique to estimate storage is through calibration, using rainfall and throughfall data and a canopy interception model, yet available models are generally useful only over long time periods (e.g., Klingaman et al., 2007; van Dijk et al., 2015; Linhoss and Siegert, 2020) because of flawed model structure (e.g., Raupach and Finnigan, 1988; Klaassen et al., 1998; Vrugt et al., 2003; Schymanski and Or, 2017). Development of better models of precipitation movement through canopies at finer spatial and temporal scales is hampered by lack of detail in the understanding of the canopy store.

Poor model performance at the event scale compromises physical interpretability of derived parameters and limits extrapolation of model predictions beyond the calibration data. In particular, data are insufficient to differentiate among competing models of the nature of the canopy store, despite multiple mutually exclusive conceptual models. For example, canopies have been treated conflictingly as stores that release no drip until some threshold storage volume (Mulder, 1985), and as stores that release drip proportionally to storage up to a threshold maximum (Massman, 1980). Because of these uncertainties, the most widely used model — that of Rutter et al. (1971) and its simplification by Gash (1979) and subsequent refinements — avoids literal description of storage and defines it only in terms of its availability for evaporation. Some modelers have even completely avoided explicitly resolving canopy storage (e.g., Liu, 1997), increasing the reliance on calibration.

Canopy storage and release is important for evaporation, but also for

* Corresponding author.
E-mail address: knanko@ffpri.affrc.go.jp (K. Nanko).
[1] Present address: Department of Geography, Miami University, Oxford, OH, USA.

https://doi.org/10.1016/j.jhydrol.2022.128144
Received 14 February 2022; Received in revised form 11 May 2022; Accepted 29 June 2022
Available online 8 July 2022

biogeochemical and ecological processes. Factors such as contact time and flow routing are important for biogeochemical transformations (e.g., Beier et al., 1993; Robson et al., 1994; Hansen, 1996; Tucker et al., 2020) and epiphyte habitat (e.g., Garth, 1964; Gauslaa, 2014). Seasonally variable biological activity and canopy phenology cause strong variations in canopy surfaces and interactions between precipitation and dry deposition or leachate from plants (Puckett, 1990; Whelan et al., 1998; Michalzik et al., 2016; Klamerus-Iwan and Witek, 2018). Poor representation of canopy storage and release means that canopy interception models cannot be used to make inferences to these related processes.

Improving models of canopy storage, routing, and release requires novel data. Estimates of storage have been nearly universally based on coupled observations of rainfall and throughfall, and both evaporation and storage are typically unmeasured. The difficulties in making direct observations of evaporation and storage mean that indirect inference will likely still be required into the future, but new ways to characterize throughfall may improve insights into canopy processes. For example, better detail about time-varying throughfall rates can improve understanding of dynamic storage, drip, and evaporation (Keim and Link, 2018), and the use of chemical tracers in throughfall has similarly yielded insights (Allen et al., 2017; Herbstritt et al., 2019).

One throughfall characteristic that has great potential to reveal canopy storage and release processes is the drop size distribution (DSD). The DSDs of throughfall are different from the DSDs of the rainfall because canopies partition throughfall into free throughfall, splash throughfall, and canopy drip components (Moss and Green, 1987; Nanko et al., 2006; Levia et al., 2019; Zhu et al., 2021). For foliated trees, canopy drip generally constitutes the largest volumes (Levia et al., 2019). Vegetative surface characteristics and topology, especially inclination, shape, surface roughness, the presence of trichomes on leaves, and surface hydrophobicity generate characteristic throughfall DSDs (Nanko et al., 2006; Konrad et al., 2012; Nanko et al., 2013; Levia et al., 2017; Levia et al., 2019; Lüpke et al., 2019; Pinos et al., 2020). Vegetative surfaces and water retention characteristics change with seasons (e.g., Klamerus-Iwan and Błońska, 2016), and thus DSDs likely also vary through time. The differing influences of foliar and woody surface flowpaths and subsequent drip points on throughfall DSD (e.g., Nanko et al., 2016; Levia et al., 2019) present an opportunity to examine any effects of canopy phenophase on intra-event changes in throughfall DSDs that may shed light on throughfall generation processes. DSDs are an important tool for understanding the nature of canopy storage because throughfall drop sizes depend on interactions with vegetative surfaces. High-energy interactions typified by momentary impact and low residence time in the canopy favor generation of splash droplets, whereas low-energy interactions typified by longer residence time in storage and drip after flow along surfaces favor generation of larger droplets. These relationships permit judicious extrapolation from the DSD to storage and residence times in the canopy.

The objective of this work is to use the phenological transition from leafed to leafless to determine the role of canopy and canopy phenophase in throughfall generation. To accomplish this, we quantified throughfall DSDs under American beech (*Fagus grandifolia* Ehrh.) trees in a forest in Maryland, USA, before, during, and after autumnal leaf senescence. We hypothesized that throughfall DSDs change within events and by canopy phenophase because flowpaths through canopies vary by canopy state. In particular, we hypothesized there are multimodal DSDs in throughfall, as opposed to unimodal DSDs for open rain. In addition, we hypothesized that DSDs of canopy drip vary through events because the generation processes of canopy drip vary through events as canopy states change. Verification of these hypotheses would be consistent with the overall hypothesis that throughfall takes multiple paths through the canopy and that these change during events and with phenophase.

2. Materials and methods

2.1. Site description and study design

The research was conducted at Fair Hill Natural Resources Management Area in northeastern Maryland, USA, at an elevation of 70 m above sea level (39° 42' N, 75° 50' W). Northeastern Maryland has warm summers and mild winters with precipitation mostly evenly disbursed throughout the year, although there is a modest increase in summer and autumn. The climate is classified as Cfa by the Köppen climate classification system. Forest vegetation is primarily second-growth. American beech, yellow poplar (*Liriodendron tulipifera* L.), red maple (*Acer rubrum* L.) and oak spp. (*Quercus*) are predominant. The particular stand examined had 233 trees ha^{-1}, mean canopy height of approximately 23 m, a mean diameter at breast height (DBH) of trees>10 cm of 39.5 cm and a stand basal area of 43.7 m^2 ha^{-1}. A woody area index of 1.21 m^2 m^{-2} and a leaf area index (LAI) of 5.12 m^2 m^{-2} was estimated by a LAI-2000 Plant Canopy Analyzer (LI-COR Biosciences, NE, USA) (Hudson et al., 2017).

The study trees occupied an intermediate layer between the understory and overstory, as is common for some beech trees as a shade tolerant species (Fig. 1). The LAI measured with a LAI-2000 Plant Canopy Analyzer above each measuring point of raindrops ranged from 1.37 to 2.21 m^2 m^{-2} on 7 November 2018 and from 0.75 to 2.11 m^2 m^{-2} on 23 January 2019. Due to litterfall, these values are lower than those of the full growing season (as listed above), representing snapshots during litterfall and then dormancy. The three study trees were in close proximity to each other. The three trees had crown base heights of 0.6, 1.2, and 1.2 m and overall tree heights of 9.4, 7.7, and 8.4 m, respectively. The distances between the three trees ranged from 8.3 to 9.5 m. Clusters of four or five disdrometers (14 in total) were positioned

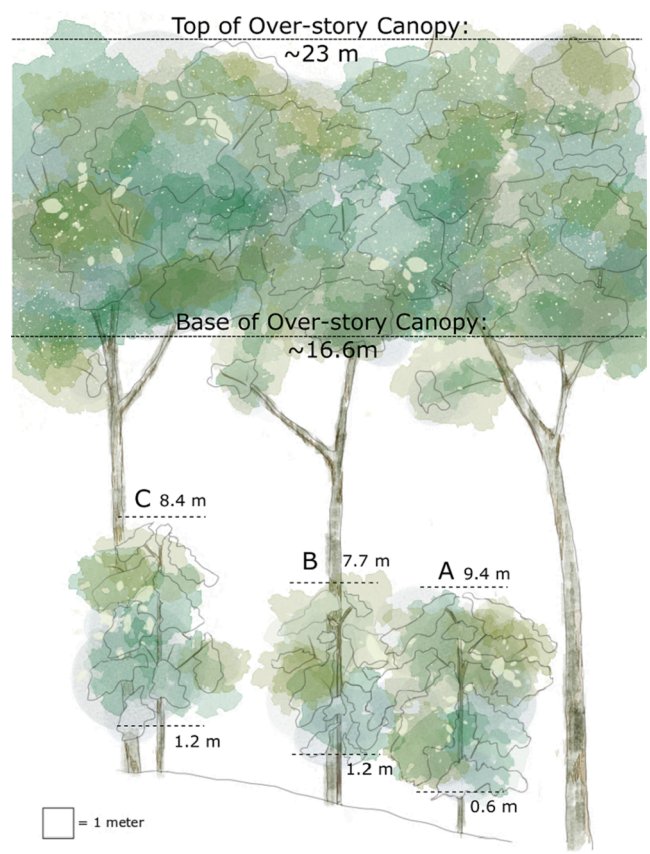

Fig. 1. Schematic diagram of the field site. The heights of the over story represent the overall average at this particular location. Scale is approximate.

(details are shown in section 2.2) 60 cm above the ground within 0.26–2.76 m (median 0.87 m) of the stem of each of the three trees to measure throughfall (TF) drops. One disdrometer for open rainfall (OP) was positioned in an open field 120 – 130 m from the under-canopy disdrometers.

2.2. Measuring raindrops and throughfall drops with laser disdrometers

The laser disdrometers used to measure raindrop size and velocity in this study were originally developed by Nanko et al. (2006) and used by Pinos et al. (2020). Each one is equipped with a pair of laser transmitters and receivers (IB-30, KEYENCE Corporation, Osaka, Japan) operated by a laser amplifier (IB-1000, KEYENCE Corporation, Osaka, Japan). Drops were measured within a 4500 mm^2 sampling area (30 mm wide and 150 mm long horizontally) with 1 mm thickness of the laser beam. When a drop passes through the laser beam, the laser beam is ablated and the output voltage from the amplifier decreases in proportion to the intercepted area of the laser beam. The output voltage (0–5 V) from the laser amplifier was collected by a micro-controller unit (Arduino UNO) every 50 μs (20 kHz) with 12-bit A/D converting and recorded. The output voltage data were converted into drop diameter and velocity data (Pinos et al., 2020). While Arduino based datalogging systems are cost effective and flexible, they are not without their limitations. The Arduino logging system cannot record data for all drops that pass through sampling area (Pinos et al., 2020). The hardware specifications, chiefly a limited sampling rate, introduce uncertainty under the following circumstances, drops with diameter < 0.8 mm, a continuous stream of raindrops or throughfall drops (an unlikely occurrence) and several drops entering the sampling area simultaneously. To overcome this, a filtering procedure is used to exclude the unreliable data (Section 2.3).

Raindrops and TF drops were observed from 26 October to 26 December 2018. Nine rain events were obtained with preceding dry intervals of>6 h. For five of the nine rain events, drop data were collected in both OP and TF (Table 1).

2.3. Data analysis

Some of the drop data were removed before data analysis because of instrumental detectability or implausibility. The first filter was to eliminate drop diameters < 0.8 mm (3.6% in number and 0.6% in volume of the recorded data) because the system could not reliably identify voltage decreases affiliated with these small drops (Pinos et al., 2020). For open rainfall, the volume fraction of drops with diameter < 0.8 mm was ~ 41% at rainfall intensity of 1 mm h^{-1} and ~ 15.5% for intensity of 10 mm h^{-1} based on the estimated DSDs by Marshall and Palmer (1948). The second filter was to eliminate drop diameter > 10.0 mm (although there were none in this study) because 10 mm was assumed the maximum raindrop size and larger voltage drops are likely affiliated with multiple drops instead of only one. The third filter was drop velocity > 12 m s^{-1} (0.2% in number and 2.2% in volume of the recorded data) because the velocity was implausibly much higher than terminal velocity. The fourth filter was drop velocity less than the theoretical velocity from a fall of < 0.5 m (Laws, 1941) (6.2% in number and 3.9% in volume of the recorded data); these errors likely originated from drops fallen from the disdrometer itself or objects other than drops passing through the laser beam. After applying the filters, the volume sum of disdrometer measured drops was 39% less than the totals collected below each disdrometer, which is the same underestimate reported by Pinos et al. (2020). This under-representation of splash droplets means that the data were best suited to analysis of canopy drip. After the filters, the drop data were post-processed into 1-min intervals and 0.1-mm diameter classes. Rainfall and TF amounts were calculated from the volume of the measured drops and sampling area of the laser disdrometers.

Throughfall was partitioned into free throughfall (FR), splash throughfall (SP), and canopy drip (DR) by drop-size class, using simultaneous 1-min interval DSDs of both OP and TF, as described by Levia et al. (2019) and applied by Nanko et al. (2020) and Pinos et al. (2020). The partitioning in this study followed the protocol of Pinos et al. (2020), assuming the maximum diameter of SP was 2.0 mm and the minimum diameter of DR was 1.0 mm. Throughfall volume was thus assumed to vary by drop-size class d (mm) at each 1-min interval t ($TF_{d,t}$) as the sum of $FR_{d,t}$, $SP_{d,t}$, and $DR_{d,t}$:

$$TF_{d,t} = \begin{cases} FR_{d,t} + SP_{d,t} : d < 1.0 \\ FR_{d,t} + SP_{d,t} + DR_{d,t} : 1.0 \le d < 2.0 \\ FR_{d,t} + DR_{d,t} : d \ge 2.0 \end{cases} \quad (1)$$

$FR_{d,t}$ was calculated as:

$$FR_{d,t} = p_t OP_{d,t} \quad (2)$$

where p_t is the free throughfall fraction (dimensionless, from 0 to 1) in each 1-min interval, assumed to be the maximum value across all d for which $(TF_{d,t} - p_t OP_{d,t}) > 0$. $SP_{d,t}$ [$d \le 1.0$ mm] and $DR_{d,t}$ [$d \ge 2.0$ mm] were calculated by mass balances in the ranges of Eq. (1) where they were assumed to be the only non-FR components of throughfall. $SP_{d,t}$ [$1.0 \le d < 2.0$ mm] was determined by the Weibull cumulative distribution function with Weibull coefficients fitted for each 1-min interval, and $DR_{d,t}$ [$1.0 \le d < 2.0$ mm] then determined from mass balance. Furthermore, $DR_{d,t}$ was partitioned into four drop size classes, $DR_{d,t\_<4.0}$, $DR_{d,t\_4.0\text{-}5.5}$, $DR_{d,t\_5.5\text{-}6.6}$, and $DR_{d,t\_6.6<}$, whose subscript indicates diameter (mm).

Table 1
Statistical summary of rainfall and throughfall drop parameters.

Event	Start date in 2018	Duration (h) [a]	OP (mm) [b]	TF (mm) [c]	Number of OP drops (count 4500 mm^{-2})	Number of TF drops (count 4500 mm^{-2}) [d]
1	26 October	22.3	19.2	17.8 [12.3, 24.3]	76,541	41,724
2	9 November	30.4	11.3	9.7 [7.8, 14.2]	45,250	24,520
3	12 November	28.5	16.1	16.1 [12.0, 28.0]	98,510	52,944
4	24 November	29.5	37.0	29.8 [23.9, 44.1]	95,440	75,983
5	14 December	39.9	24.1	20.9 [18.2, 31.5]	116,383	77,733

[a] Duration from first raindrop to last raindrop in OP.
[b] Open rainfall amount measured by a laser disdrometer.
[c] Mean [minimum, maximum] of the 14 laser disdrometers.
[d] Mean count by the 14 laser disdrometers.

3. Results

3.1. Drop size and velocity at the event and intra-event scales with phenophase

At the event and intra-event scales, throughfall drops varied by phenophase as leaves abscised and fell from October to December (Figs. 2 and 3). Larger drops were observed in TF than OP. For example, the maximum drop size in OP was <5 mm in the events of October 26 and December 14, but many TF drops were >5 mm and some were 7–9 mm (Fig. 2b and 3b). In the leafless phenophase, there was a gap in the TF-DSD near 6.5 mm (Fig. 3b) that was not present with leaves on

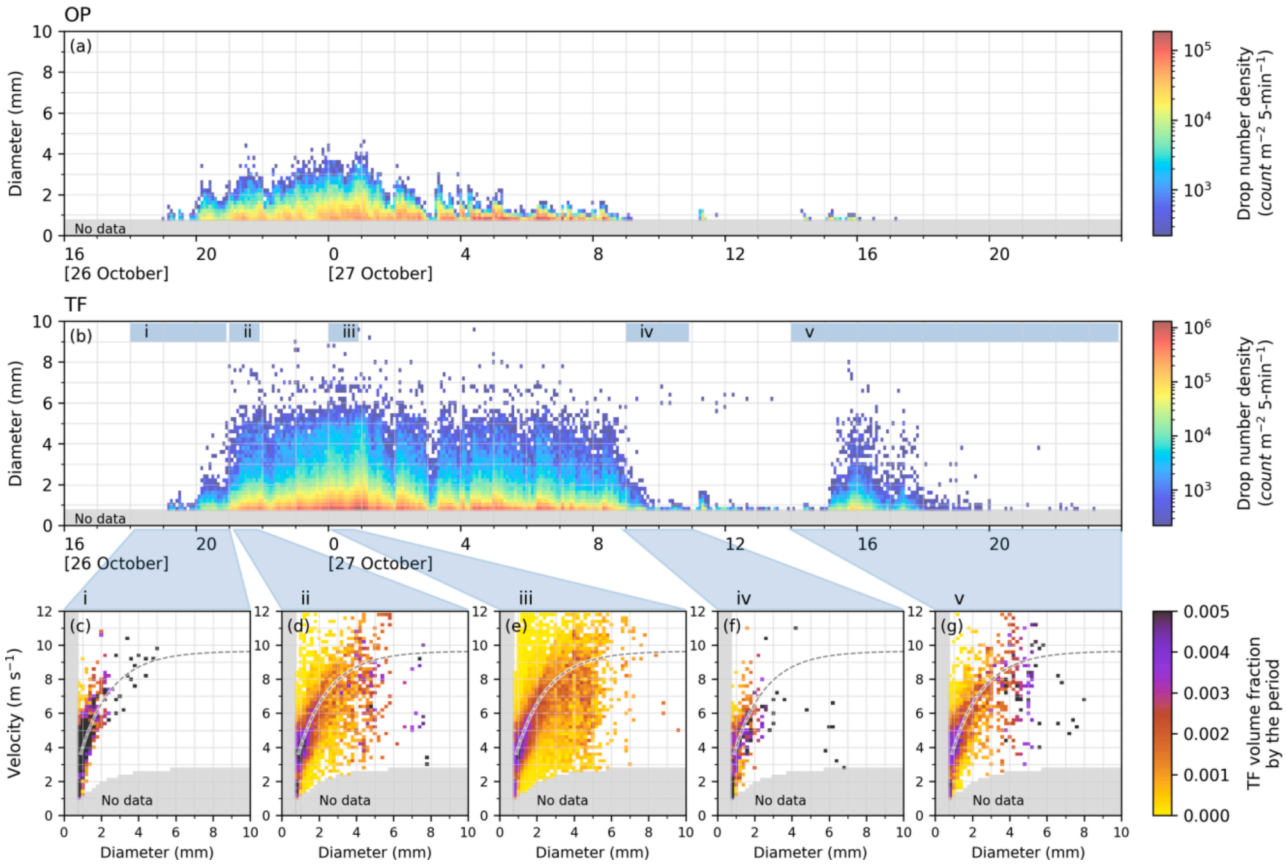

Fig. 2. Temporal variation of drop size and velocity during the 26–27 October 2018 rain event during the leafed phenophase, showing number-based drop size distributions at resolution of 5 min and 0.2 mm diameter for (a) OP and (b) TF, and (c-g) volume-based drop size-velocity distributions at resolution of 0.2 mm diameter and 0.2 m s^{-1} velocity class during the five periods shown in (b). TF data are based on the sum of all 15 subcanopy disdrometers. Dashed lines (c-g) indicate terminal velocity. Gray shading indicates undetectable drops with diameter < 0.8 mm and theoretical velocity from a fall of < 0.5 m.

(Fig. 2b). At the cessation of OP, TF was still observed, and the time lag between the last drops in OP and TF was shorter in the leafless phenophase (Fig. 3a,b) than the leafed phenophase (Fig. 2a,b).

The relationship between the diameter and the velocity of TF drops changed within events. At the beginning of events, most of the TF drops were near terminal velocity, which is the theoretical velocity for OP drops (Fig. 2c and 3c). After the canopy began to generate DR throughfall, larger drops than the maximum size of OP drops were observed with various velocities (Fig. 2d-g and 3d-g). During periods of higher rain rates, TF was composed of drops with various sizes and velocities (Fig. 2e and 3g). In the absence of OP, velocities of large TF drops were slower (Fig. 2f and 3f).

3.2. Drop size distributions (DSDs) among rain events

Throughfall-DSDs varied with phenophase (Fig. 4). In contrast with OP, in which DSDs were unimodal (Fig. 4a), DSDs of TF were multimodal, with peaks at 1.2 mm, 4–5 mm, and 6.8 mm (Fig. 4b). TF volume in the 5.5–6.6 mm diameter class was lower than surrounding diameter classes (Fig. 4b). DR-DSDs indicated that DR was partitioned into four drop size classes: $DR_{<4.0}$, $DR_{4.0\text{-}5.5}$, $DR_{5.5\text{-}6.6}$, and $DR_{6.6<}$ (Fig. 4c).

The TF-DSD in diameter <2 mm corresponded with the OP-DSD (Fig. 4a,b). Two events (12 November and 14 December) had smaller OP-DSDs compared with the other three events (Fig. 4a). Both events had higher TF volume ratio in diameter < 2 mm (Fig. 4b).

As for $DR_{4.0\text{-}5.5}$, a higher volume ratio was observed in the first three events (before mid-November), whereas a lower volume ratio was observed in the last two events (after late November) (Fig. 4c). The diameter at the peak of $DR_{4.0\text{-}5.5}$-DSD became larger with the procession of the phenophases. The diameter at the peak of each event was 4.4, 4.5, 4.9, 4.9, and 5.0 mm for each of the five sampled rain events, respectively (Fig. 4c).

As for $DR_{6.6<}$, the shape of the DSDs was similar among the events. The total volume ratio in each event was 0.030, 0.040, 0.063, 0.048, and 0.049, respectively.

With respect to $DR_{5.5\text{-}6.6}$, the total volume ratio of $DR_{5.5\text{-}6.6}$ decreased with the procession of the phenophases, with values of 0.031, 0.023, 0.021, 0.010, and 0.013 in successive rain events and the canopy progressing toward a leafless state, respectively.

3.3. Throughfall generation processes

The proportion of OP represented by each of the inferred TF types (FR, SP, and four DR size classes) changed as OP accumulated in each event (Fig. 5). During the initial 5 mm of OP (Fig. 5f-j), TF increased as a proportion of OP and did not reach a stable phase. The proportion of OP partitioned into FR also increased through the first 5 mm of OP in the first two events (greater leaf cover), but reached a stable phase in last three events (decreasing leaf cover). The proportion of OP partitioned into SP also increased through the first 5 mm of OP in the first three events (greater leaf cover), but was higher at the beginning of the event and afterward decreased and stabilized in last two events (decreasing leaf cover). The proportions of OP categorized as $DR_{<4.0}$ and $DR_{4.0\text{-}5.5}$ also increased through the first 5 mm of OP in all events (but approaching stability in later events), while the proportions of OP categorized as $DR_{5.5\text{-}6.6}$ and $DR_{6.6<}$ were relatively stable after being first generated.

Over the course of entire events, the TF volume ratio by OP varied by

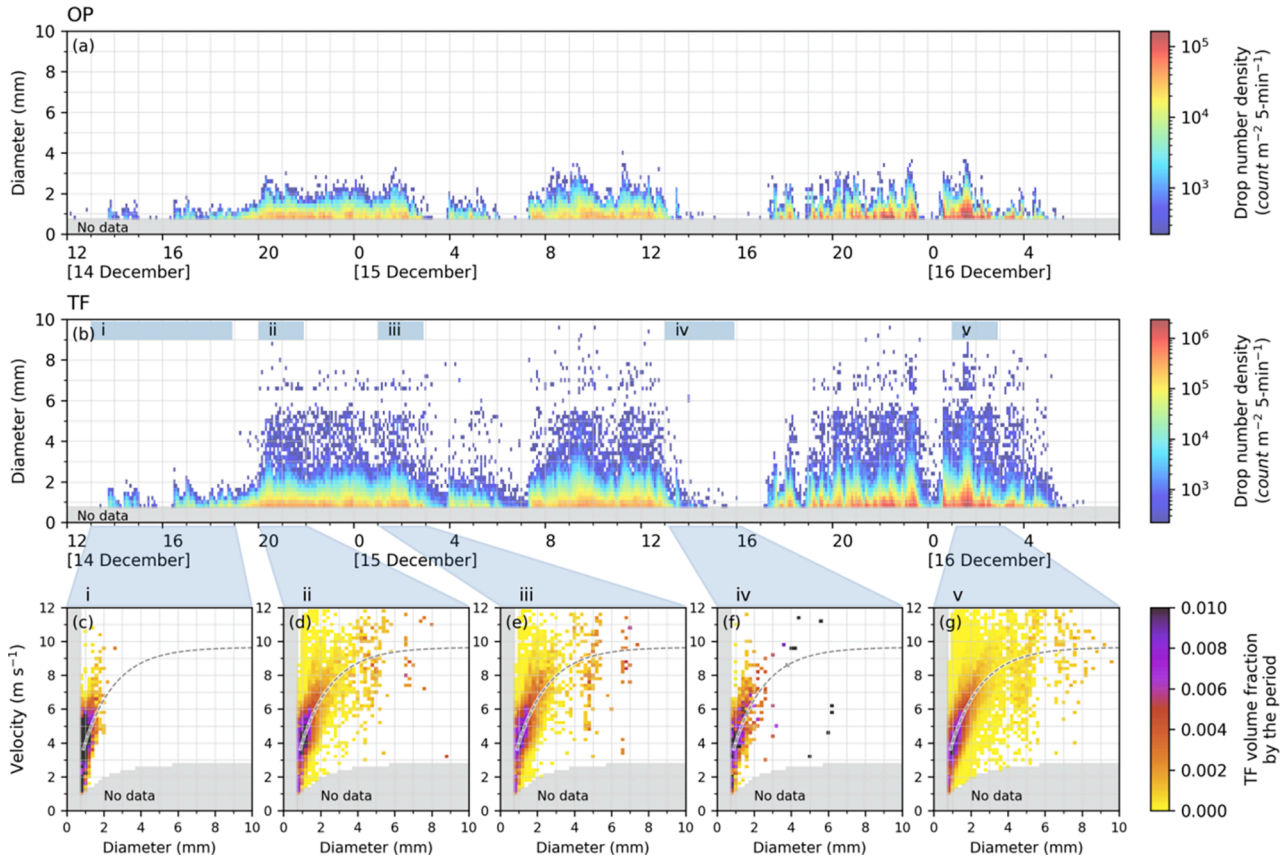

Fig. 3. Temporal variation of drop size and velocity during the 14–16 December 2018 rain event during the leafless phenophase, showing number-based drop size distributions at resolution of 5 min and 0.2 mm diameter for (a) OP and (b) TF, and (c-g) volume-based drop size-velocity distributions at resolution of 0.2 mm diameter and 0.2 m s^{-1} velocity class during the five periods shown in (b). TF data are based on the sum of all 15 subcanopy disdrometers. Dashed lines (c-g) indicate terminal velocity. Gray shading indicates undetectable drops with diameter < 0.8 mm and theoretical velocity from a fall of < 0.5 m.

event (Fig. 5a-e). More OP was necessary for TF volume ratio by OP to reach a stable phase in earlier events (leaf on): >5 mm of OP was necessary to reach a stable phase on 26 October (Fig. 5a), but around 5 mm of OP on 14 December (Fig. 5d,e). After a stable phase, TF volume ratio by OP did not always remain stable. In the first three events (greater leaf cover), TF volume ratio by OP increased in the end of the event or mid-event (Fig. 5a-c). Drop-size distributions during these periods were dominated by $DR_{<4.0}$, $DR_{4.0\text{-}5.5}$, and $DR_{6.6<}$. The proportion of OP partitioned into FR and SP tended to increase with accumulating OP in the 26 October event, but changed little during the 9 and 12 November events once the stable phase was reached.

In the last two events (decreasing leaf cover), the proportion of OP partitioned into DR was largely constant in the stable phase of TF (Fig. 5d,e). TF volume ratio by OP decreased after an initial stable phase in 24 November (Fig. 5d). This change was dominated by decreases in FR and SP, not by decreases in DR.

The variability of TF volume ratio by OP at the TF measuring points among the rain events varied through the phenophase transition (Fig. 6). As leaf cover decreased, the proportion of OP partitioned into FR and SP increased, $DR_{<4.0}$ and $DR_{4.0\text{-}5.5}$ decreased, and $DR_{6.6<}$ slightly increased.

The OP amount required to initiate DR did not clearly vary across the phenological transition (Fig. 6g-j), although there is some evidence that the smallest canopy drips were slightly delayed at the beginning of events with more leaves. More OP was necessary to generate larger DR drops across phenophases.

To reach 50% of maximum volume ratio (a more stable estimate than the OP necessary to reach the maximum), more OP was generally necessary for larger DR (Fig. 6k-p). With the phenophase transition to leaf-off, less OP was necessary for FR, SP, $DR_{<4.0}$, and $DR_{4.0\text{-}5.5}$ but no clear trends were found for generation of $DR_{5.5\text{-}6.6}$ and $DR_{6.6<}$ across the phenophase transition.

4. Discussion

4.1. Leaf flowpaths and branch flowpaths

Not all canopy flowpaths or drip points are equal. In fact, per our hypothesis, we found that TF-DSDs are multimodal and vary at both intra-event and inter-event scales as well as with phenophase for flowpaths ending at foliar or structurally-mediated woody surface drip points. Transformations of drop sizes from those of open rainfall to those of throughfall give several important clues regarding the flowpaths that created the characteristic DSDs in throughfall. Leaf flowpaths were apparently important for drops < 5.5 mm because drops smaller than that decreased by 1/3 as the leaves dropped (Fig. 4c). Branch flowpaths ending at structurally-mediated woody surface drip points appeared to be more important for the largest drops > 6.6 mm because the proportion of drops of that diameter increased by 1.6 times as leaves dropped (Fig. 6f) and exposed branches to more direct rainfall. Overall, our data suggest that throughfall routed to the forest floor from foliar surfaces generated smaller-sized DR with more canopy drip generating points and shorter residence time as compared to throughfall last in contact with branch surfaces at structurally-mediated woody surface drip points. Nanko et al. (2016) and Levia et al. (2019) witnessed the same phenomenon whereby the largest diameter canopy drip was generated at structurally-mediated woody surface drip points.

Based on the association of throughfall drop sizes with these two flowpaths, we suggest a conceptual model of canopy residence time, in

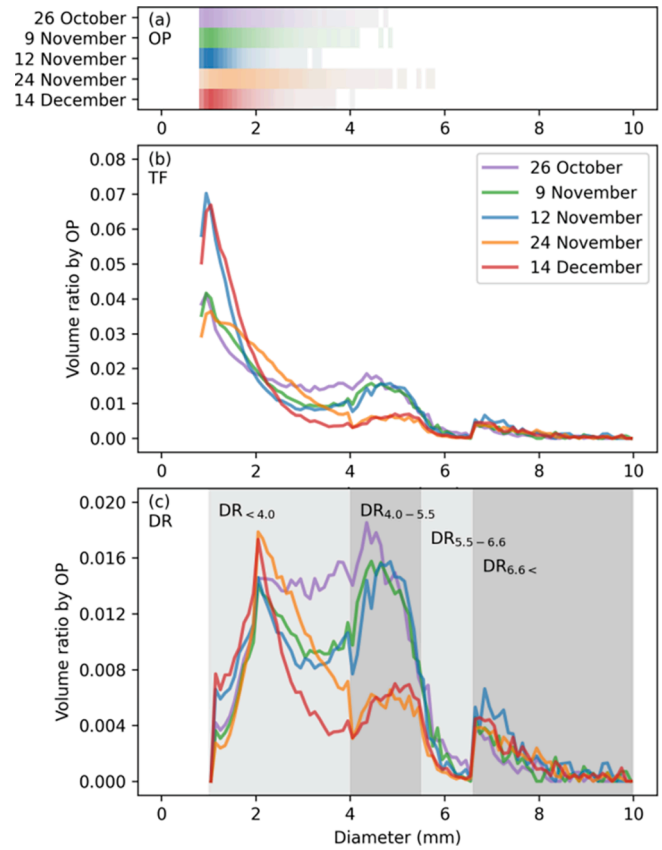

Fig. 4. Volume-based drop size distributions (DSDs) for every 0.1-mm diameter class for five rain events of (a) open precipitation, (b) throughfall and (c) canopy drip. OP-DSD is shown by color intensity. TF-DSD and DR-DSD are the average of all of TF laser disdrometers' data. Gray bands in DR-DSD denote the groups of DR partitioned by drop diameter.

which flowpath development depends on canopy characteristics (Fig. 7). Short-residence flowpaths are probably mostly composed of leaf flowpaths because leaves tend to be more hydrophobic than branches and hydrophobic surfaces store less water (Holder, 2013). These shorter-residence flowpaths are apparently generally composed of smaller DR, as indicated by greater dominance of small drops in the leaf-on portion of our dataset (Fig. 4c and 6c-d). The number of short-residence flowpaths is therefore related to the amount of leaves. Conversely, medium- and longer-residence flowpaths are apparently mostly branch flowpaths, as evidenced by relatively stable generation of larger DR across the entire phenological transition. The generation of branch DR is especially pronounced at structurally-mediated woody surface drip points (e.g., irregular rough points, branch concavities), which is related to branch architectural characteristics (Crockford and Richardson, 2000; Herwitz, 1987). More rainwater is required to generate branch DR than leaf DR (Fig. 6g-j and 6 m-p), likely because larger local storage capacities of bark are typically higher than leaves (Campellone et al., 2020).

It is important to draw a distinction between occasional woody surface drip points and structurally-mediated woody surface drip points that tend to generate the largest median drip diameters (Levia et al. 2019). In essence, due to adhesive forces, especially on saturated branches, branchflow has a longer residence time and then accumulates more water volume as it is transported down the branch to a structurally-mediated woody surface drip point, where momentum transfer of incoming branchflow outweighs adhesive forces and produces larger diameter drops in greater volumes. In contrast, the initiation of canopy drip along the branch sometimes could be induced by wind (or other (a)biotic mechanism) or sometimes along a wetting front as the branch attains saturation at an occasional woody surface drip point. Occasional woody surface drip points tend to be spatially and temporally transitory, while structurally-mediated woody surface drip points tend to be fixed as they occur at specific locations once branch flowpaths are saturated (Herwitz, 1987; Levia et al., 2019). Canopy drip generated at an occasional woody surface drip point is of smaller diameter and volume than the canopy drip originating from structurally-mediated woody surface drip points, or even foliar drip points in many cases (Levia et al., 2019). It is important to note that the range of canopy drip diameters between foliar drip points and woody surface drip points overlap and, depending on local conditions (e.g., timing within a discrete event, wind, species), they may be more or less equal or one could exceed the other. Structurally-mediated woody surface drip points may sometimes be amplified or dampened by foliage.

4.2. *Intra-event variation of canopy flowpaths*

From the evolution of drop sizes in throughfall, we infer that canopy flowpaths vary throughout the progression of rain events. This intra-event variation of canopy flowpaths must be at least partly attributable to vertical wet-up of the canopy, especially for our sample trees positioned between the under- and overstory. At the onset of the event, throughfall is mostly composed of FR and SP and less DR. Initial rain intercepted by the canopy mostly wets the upper canopy and starts to develop leaf and branch flowpaths. Soon, as flowpaths in the upper canopy layer develop, canopy drip from shorter-residence flowpaths begins, and drip points higher in the canopy generate DR sooner than lower portions of the canopy. A crucial piece of evidence supporting this interpretation in our data is drop velocity. Approximately 12 – 14 m is necessary for drops of the size we measured to reach terminal velocity (Wang and Pruppacher, 1977); canopy height was approximately 23 m, so only DR generated from the upper half of the canopy could obtain terminal velocity as we observed. DR generated from the canopy at heights of < 12 m would not reach terminal velocity. As for water drops with a 5-mm diameter, fall velocities would have reached 9.25, 8.86, and 4.27 m s^{-1} with fall heights of 20, 5, and 1 m, respectively (Laws, 1941).

Progressive wet-up of lower canopy layers occurs by rainfall directly or by SP and DR routed from upper layers. The progress of canopy wet-up apparently increases the number of leaf flowpaths in all canopy layers and starts to generate branch flowpaths. The evidence for this is that larger DR did not initiate early in events, indicating that these pathways always required substantial wet-up (Fig. 2b, 3b, and 6 g-j). Saturated branch pathways may route to stemflow all the way to the soil surface (Dunkerley, 2014), but some stemflow pathways typically result in drip from the branch surface.

The conceptual model we present here is consistent with and helps explain observations in previous observations of throughfall drop generation and stemflow. Consistent with our conceptual model of progressive wetting, Nanko et al. (2008, 2011) found that the mean velocity of DR was lower from a saturated canopy than one undergoing canopy wetting. This likely means that a saturated canopy generated DR from various canopy layers instead of only the higher layers typical of DR from wetting canopies. Another key conclusion from our research is that wetter canopies generate larger DR at structurally-mediated woody surface drip points along branch flowpaths. This conclusion is consistent with experimental observations that such woody surface drip points generate larger DR than foliar surfaces (Nanko et al., 2016; Levia et al., 2019). The DR-DSDs are affected by canopy architecture, water repellency, and inclination of the plant surfaces (Konrad et al., 2012). Experimental work has consistently shown that bark surfaces are usually rougher (Campellone et al., 2020) and more hydrophilic (i.e., less water repellent) than leaves (Herwitz, 1987), both of which promote the retention of water in longer-residence flowpaths. Levia et al. (2019) showed the volume fraction of DR increased most gradually for coniferous species from the onset of simulated rain events during an indoor rainfall simulation.

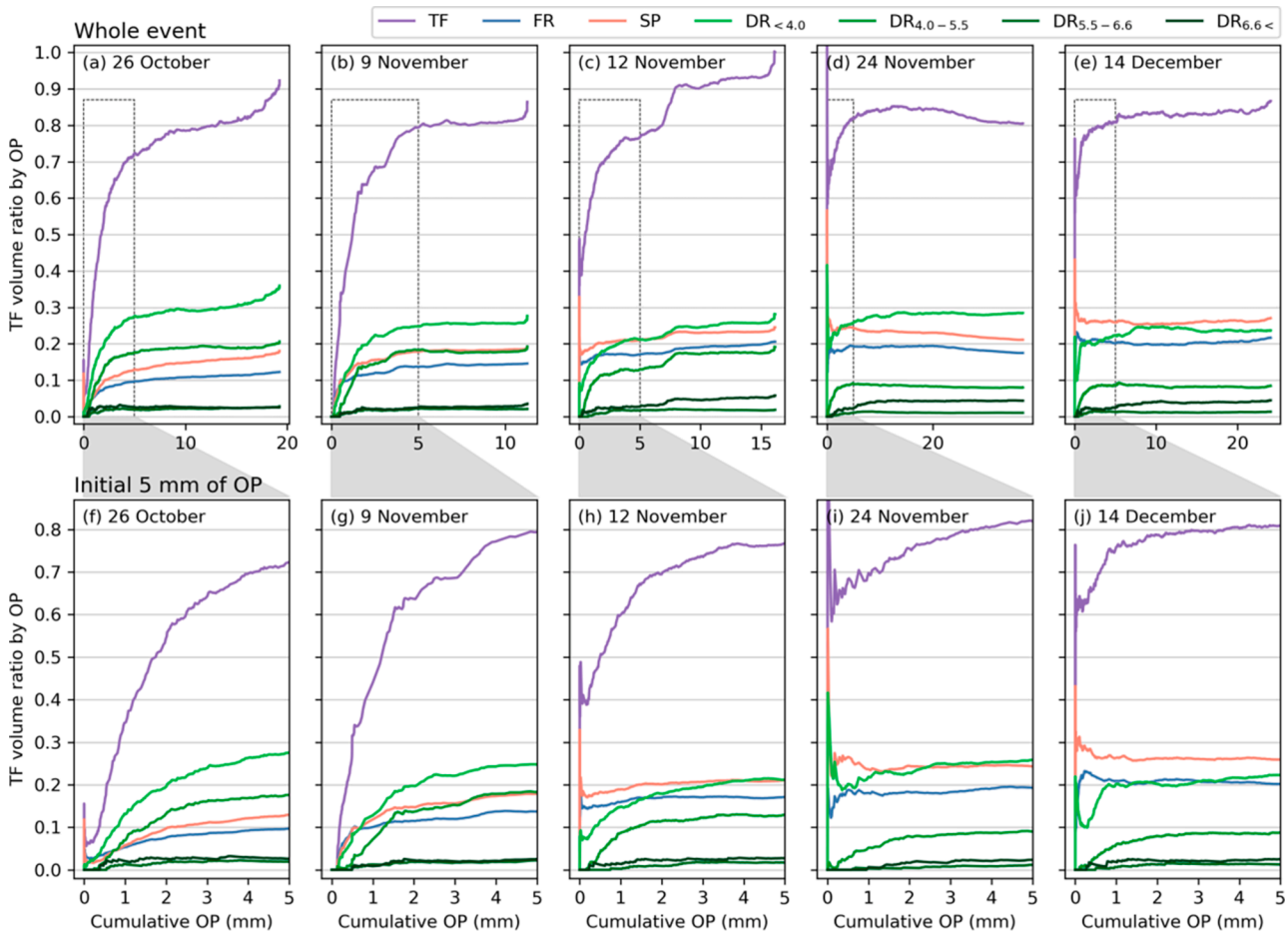

Fig. 5. Relationship between cumulative OP and cumulative volume ratio of each TF type by OP for the five rain events for (a-e) whole rain event and (f-j) initial 5 mm OP. The four groups of DR are shown in Fig. 4.

When rain ceases, the top canopy layer generates progressively fewer DR as storage empties, but the lower canopy layers continue to generate longer DR by the supply of water via leaf and branch flowpaths from above. This is why TF continues after the end of rainfall. There are likely nonlinearities and thresholds in the relationships between precipitation characteristics and flowpaths. Rainfall intensity, drop sizes, and wind affect momentum of rainfall, which therefore affects detention on vegetation (Aston, 1979; Calder et al., 1996; Hörmann et al., 1996; Keim et al., 2006) and the generation of stemflow (Herwitz, 1987; Zhang et al., 2021).

4.3. Seasonal variation of canopy flowpaths

Canopy flowpaths vary seasonally because of varying canopy morphology. During the foliated season, our observations are consistent with the conclusion that DR is generated more by drip points along leaf flowpaths and less by drip points along branch flowpaths. With leaf abscission, more rain fell directly on woody surfaces, initiating longer-residence, branch flowpaths. DR by leaf flowpaths decreased during leaf fall, and finally leaf flowpaths disappeared. DR during the unfoliated season was mostly generated at structurally-mediated woody surface drip points along branch flowpaths. This transformation is supported by the observation that the sizes of DR became larger through the phenological transition ($DR_{<4.0}$ and $DR_{4.0\text{-}5.5}$ in Fig. 4c and 6c-d). In addition, DR-DSDs are influenced by plant surface traits, especially leaf inclination and surface hydrophobicity (Konrad et al., 2012; Nanko et al., 2013; Nanko et al., 2016). Hydrophilic leaves generated larger DR than hydrophobic leaves (Nanko et al., 2013). Although we do not have data spanning the entire growing season, it may be that the leaf-generated drops we observed were larger than those generated in the early growing season: Klamerus-Iwan & Błońska (2017) showed that leaf surface hydrophobicity decreased for *Quercus robur* as leaf surfaces changed over the course of the growing season.

As leaves fell, our results show that more FR reached the forest floor, but the proportion of FR we estimated was lower than the canopy openness we measured. As leaves fell, FR volume ratio by OP increased from 0.1 to 0.2, but clearly leaves accounted for>10% of the initial contacts with rainfall when the canopy was in full leaf. Median canopy openness estimated by LAI-2000 was 0.187 on 7 November and 0.328 on 23 January, respectively. These values are relatively higher than FR volume fractions by OP. The most likely reason that our estimates of FR were only 55–60% of the FR expected by canopy gaps is that rainfall is generally inclined by wind and therefore experiences a non-vertical pathway through the canopy that is more likely to be intercepted by plant surfaces. When estimating FR ratio from canopy coverage, raindrop inclination, wind direction, and three-dimensional canopy coverage should therefore be considered, and vertical gap measurements are likely to be overestimates of FR.

Although our data on splash droplets was limited by detectability problems below drop sizes of 0.8 mm, we nonetheless observed more SP (on the basis of cumulative drop volume) reaching forest floor with defoliation. The likely explanation for this is differences in the way SP is generated between leaves and branches. The sizes of SP depend on surface and drop characteristics (Yarin, 2006). When a raindrop impacts a leaf, less water is detained on the surface and more splash droplets are generated compared to impact onto a branch (Herwitz, 1987). On the

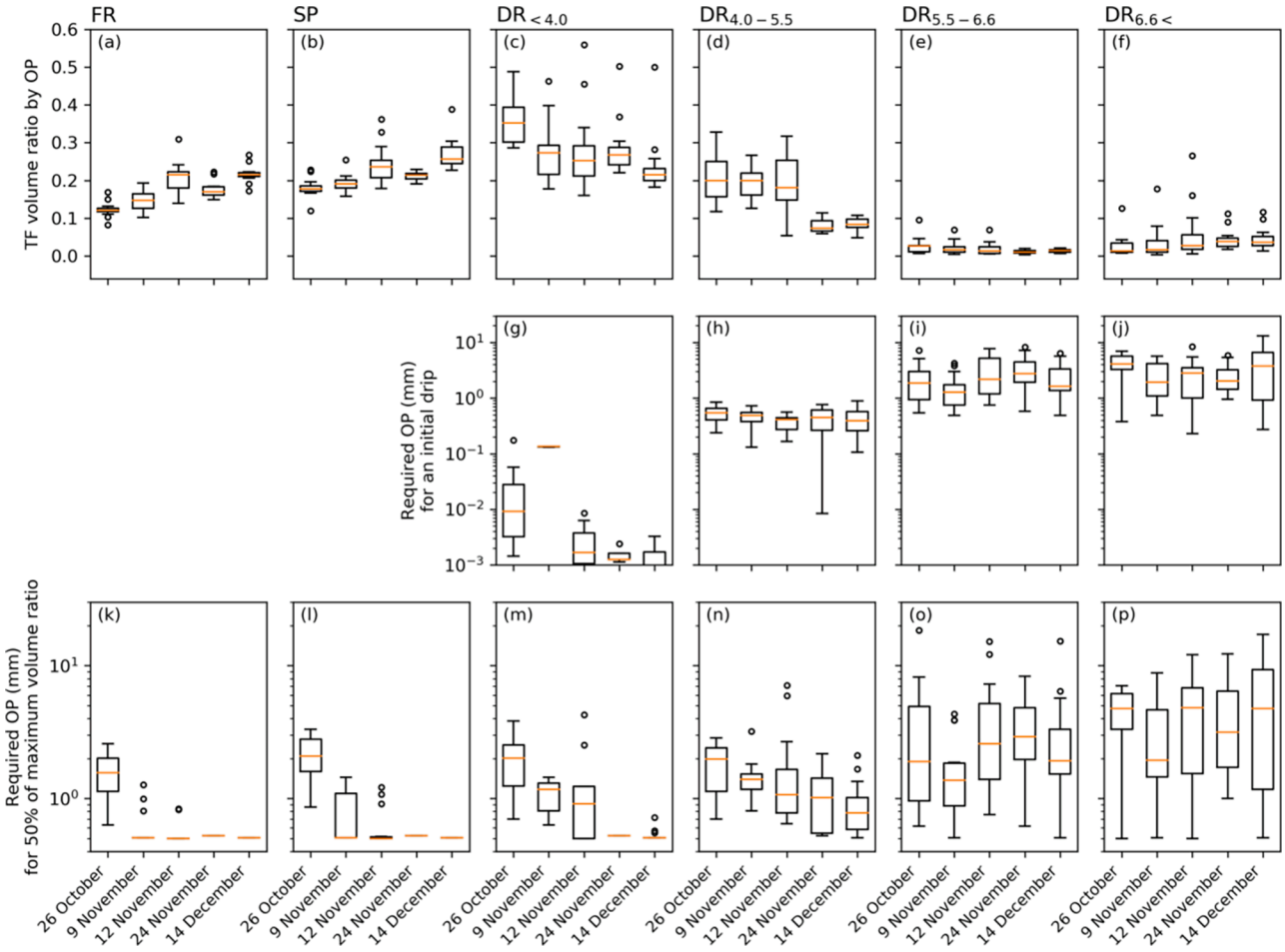

Fig. 6. Boxplots of all of TF measuring points to show difference of TF type generation among rain events. (a-f) the volume ratio by OP, (g-j) the required OP amount for an initial drip, (k-p) the required OP amount for 50% of maximum volume ratio. Orange line within the box denotes median, the upper and lower boundaries of the box denote the first and the third quantiles, respectively, the whiskers denote the extension from the box by < 1.5 times the inter-quartile, and the dots denote the data past the end of the whiskers.

other hand, leaves are more elastic than branches, and a part of the kinetic energy of a drop is converted into elastic energy (Ginebra-Solanellas et al., 2020; Holder et al., 2020; Lauderbaugh et al., 2021; Konrad et al., 2021), and thus, energy available for generating splash decreases and fewer splash droplets are generated. If the surface wettability is same, the less-elastic organs generate more SP than more elastic ones (Roth-Nebelsick et al., 2022). The balance of wettability between leaves and branches, and vertical structures of canopy layers could be responsible for the seasonal change in SP amount. It is an open question whether the same phenomenon would be observed in fine droplets.

5. Conclusions

This study advanced our understanding of canopy storage and throughfall generation by utilizing a dense network of disdrometers at the intra-event-scale to examine the interrelationships among canopy phenophase and throughfall DSD. This study has revealed the seasonal variation of the throughfall generation process based on simultaneous raindrop measurements at 14 points under the test trees. From previous work, we know that DSDs reveal partitioning into free throughfall (FR), splash throughfall (SP), and canopy drip (DR). Based on previous work on DSD generation and on the changes in DSDs we observed through the phenological transition, we inferred that DR was separated into DR from leaves and branches based on the sizes of DR. The hypotheses that throughfall DSDs changes within events and by canopy phenophase and throughfall had multimodal DSDs due to various generation processes of canopy drip through events as canopy states change were supported. We infer that flowpaths ending at foliar drip points had shorter residence times and generated smaller DR at more drip points. In contrast, we infer that branch flowpaths terminating at structurally-mediated woody surface drip points had longer residence time that generated larger DR. Leaf flowpaths decreased and branch flowpaths increased with the leaf senescence and the transition to a leafless canopy. Throughfall drop size distribution data provide novel information that can be utilized to clarify the dynamics of canopy rainwater storage and drainage.

CRediT authorship contribution statement

Kazuki Nanko: Conceptualization, Methodology, Validation, Investigation, Writing – review & editing, Funding acquisition, Software, Formal analysis, Writing – original draft, Visualization, Data curation, Supervision, Project administration, Resources. **Richard F. Keim:** Conceptualization, Writing – review & editing, Writing – original draft, Visualization, Supervision. **Sean A. Hudson:** Investigation, Writing – review & editing, Visualization, Resources. **Delphis F. Levia:** Conceptualization, Methodology, Investigation, Writing – review & editing, Funding acquisition, Writing – original draft, Visualization, Supervision, Project administration, Resources.

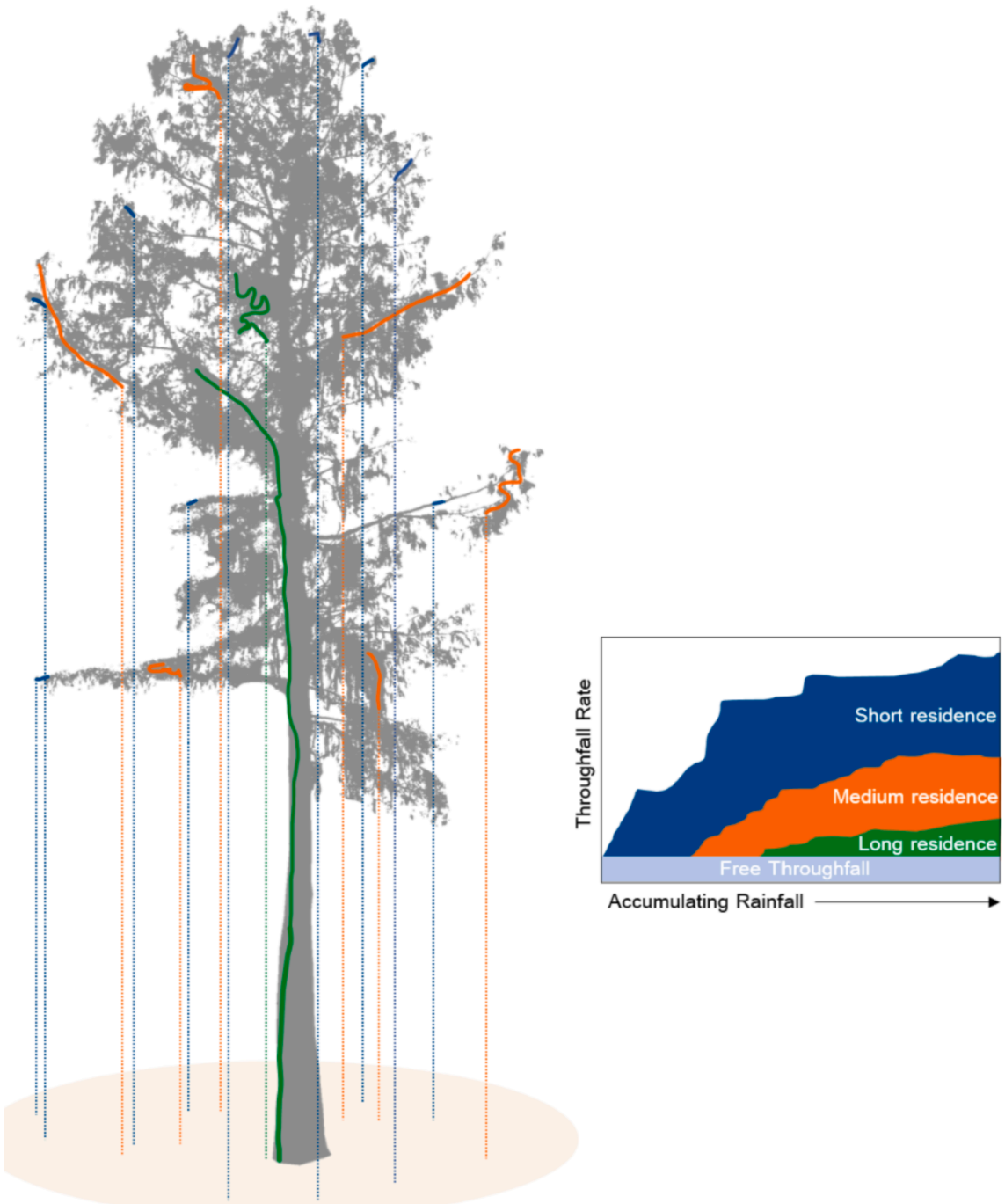

Fig. 7. Conceptual diagram of flowpath genesis and development in canopies. Shorter-residence flowpaths (blue) yield throughfall quickly, and are composed mainly of smaller drops. Medium- (orange) and longer-residence (green) flowpaths require progressively more rainfall to initiate and tend to deliver larger drops in throughfall. Residence time is likely related to, but not uniquely controlled by, flowpath length. Flowpaths may vary in residence time depending on canopy wetness or phenological phase (For interpretation of the references to color in this figure legend, the reader is referred to the web version of this article).

Declaration of Competing Interest

The authors declare that they have no known competing financial interests or personal relationships that could have appeared to influence the work reported in this paper.

Acknowledgments

The work was supported by JSPS KAKENHI [Grant numbers JP17KK0159, JP15H05626]. We are grateful to Dr. Janice Hudson, Charles Scarborough, and Justin Czech for their assistance with fieldwork.

References

Allen, S.T., Keim, R.F., Barnard, H.R., McDonnell, J.J., Renée Brooks, J., 2017. The role of stable isotopes in understanding rainfall interception processes: a review. Wiley Interdisciplinary Reviews: Water 4, e1187. https://doi.org/10.1002/wat2.1187.

Aston, A.R., 1979. Rainfall interception by eight small trees. J. Hydrol. 42, 383–396. https://doi.org/10.1016/0022-1694(79)90057-X.

Beier, C., Hansen, K., Gundersen, P., 1993. Spatial variability of throughfall fluxes in a spruce forest. Environ. Pollut. 81, 257–267. https://doi.org/10.1016/0269-7491(93)90208-6.

Calder, I.R., Hall, R.L., Rosier, P.T.W., Bastable, H.G., Prasanna, K.T., 1996. Dependence of rainfall interception on drop size: 2. Experimental determination of the wetting functions and two-layer stochastic model parameters for five tropical tree species. J. Hydrol. 185, 379–388. https://doi.org/10.1016/0022-1694(95)02999-0.

Campellone, S.V., Levia, D.F., Montalto, F.A., 2020. Differences in submillimetre surface morphology and canopy interception storage capacities of *Gleditsia triacanthos* L. (honeylocust) in relation to canopy phenophase and position. Ecohydrol 13, e2192. https://doi.org/10.1002/eco.2192.

Crockford, R.H., Richardson, D.P., 2000. Partitioning of rainfall into throughfall, stemflow and interception: effect of forest type, ground cover and climate. Hydrol. Process. 14, 2903–2920. https://doi.org/10.1002/1099-1085(200011/12)14:16/17<2903::AID-HYP126>3.0.CO;2-6.

Dunkerley, D., 2014. Stemflow production and intrastorm rainfall intensity variation: an experimental analysis using laboratory rainfall simulation. Earth Surf. Proc. Land. 39, 1741–1752. https://doi.org/10.1002/esp.3555.

Garth, R.E., 1964. The Ecology of Spanish Moss *(Tillandsia Usneoides*): Its Growth and Distribution. Ecology 45, 470–481. https://doi.org/10.2307/1936100.

Gash, J.H.C., 1979. An analytical model of rainfall interception by forests. Q. J. R. Meteorolog. Soc. 105, 43–55. https://doi.org/10.1002/qj.49710544304.

Gauslaa, Y., 2014. Rain, dew, and humid air as drivers of morphology, function and spatial distribution in epiphytic lichens. The Lichenologist 46, 1–16. https://doi.org/10.1017/S0024282913000753.

Ginebra-Solanellas, R.M., Holder, C.D., Lauderbaugh, L.K., Webb, R., 2020. The influence of changes in leaf inclination angle and leaf traits during the rainfall interception process. Agric. For. Meteorol. 285–286, 107924 https://doi.org/10.1016/j.agrformet.2020.107924.

Hansen, K., 1996. In-canopy throughfall measurements of ion fluxes in Norway spruce. Atmos. Environ. 30, 4065–4076. https://doi.org/10.1016/1352-2310(95)00444-0.

Herbstritt, B., Gralher, B., Weiler, M., 2019. Continuous, near-real-time observations of water stable isotope ratios during rainfall and throughfall events. Hydrol. Earth Syst. Sci. 23, 3007–3019. https://doi.org/10.5194/hess-23-3007-2019.

Herwitz, S.R., 1987. Raindrop impact and water flow on the vegetative surfaces of trees and the effects on stemflow and throughfall generation. Earth Surf. Proc. Land. 12, 425–432. https://doi.org/10.1002/esp.3290120408.

Holder, C.D., 2013. Effects of leaf hydrophobicity and water droplet retention on canopy storage capacity. Ecohydrology 6, 483–490. https://doi.org/10.1002/eco.1278.

Holder, C.D., Lauderbaugh, L.K., Ginebra-Solanellas, R.M., Webb, R., 2020. Changes in leaf inclination angle as an indicator of progression toward leaf surface storage during the rainfall interception process. J. Hydrol. 588, 125070 https://doi.org/10.1016/j.jhydrol.2020.125070.

Hörmann, G., Branding, A., Clemen, T., Herbst, M., Hinrichs, A., Thamm, F., 1996. Calculation and simulation of wind controlled canopy interception of a beech forest in Northern Germany. Agric. For. Meteorol. 79, 131–148. https://doi.org/10.1016/0168-1923(95)02275-9.

Horton, R.E., 1919. Rainfall interception. Mon. Weather Rev. 47, 603–623. https://doi.org/10.1175/1520-0493(1919)47<603:RI>2.0.CO;2.

Hudson, J.E., Levia, D.F., Hudson, S.A., Bais, H.P., Legates, D.R., 2017. Phenoseasonal subcanopy light dynamics and the effects of light on the physiological ecology of a common understory shrub, Lindera benzoin. PLOS ONE 12, e0185894. https://doi.org/10.1371/journal.pone.0185894.

Keim, R.F., Link, T.E., 2018. Linked spatial variability of throughfall amount and intensity during rainfall in a coniferous forest. Agric. For. Meteorol. 248, 15–21. https://doi.org/10.1016/j.agrformet.2017.09.006.

Keim, R.F., Skaugset, A.E., Weiler, M., 2006. Storage of water on vegetation under simulated rainfall of varying intensity. Adv. Water Resour. 29, 974–986. https://doi.org/10.1016/j.advwatres.2005.07.017.

Klaassen, W., Bosveld, F., de Water, E., 1998. Water storage and evaporation as constituents of rainfall interception. J. Hydrol. 212–213, 36–50. https://doi.org/10.1016/S0022-1694(98)00200-5.

Klamerus-Iwan, A., Błońska, E., 2016. Seasonal variability of interception and water wettability of common oak leaves. Annals of Forest Research 60, 63–73. https://doi.org/10.15287/afr.2016.706.

Klamerus-Iwan, A., Witek, W., 2018. Variability in the wettability and water storage capacity of common oak leaves (Quercus robur L.). Water 10, 695. https://doi.org/10.3390/w10060695.

Klingaman, N.P., Levia, D.F., Frost, E.E., 2007. A Comparison of Three Canopy Interception Models for a Leafless Mixed Deciduous Forest Stand in the Eastern United States. J. Hydrometeorol. 8, 825–836. https://doi.org/10.1175/JHM564.1.

Konrad, W., Ebner, M., Traiser, C., Roth-Nebelsick, A., 2012. Leaf surface wettability and implications for drop shedding and evaporation from forest canopies. Pure Appl. Geophys. 169, 835–845. https://doi.org/10.1007/s00024-011-0330-2.

Konrad, W., Roth-Nebelsick, A., Kessel, B., Miranda, T., Ebner, M., Schott, R., Nebelsick, J.H., 2021. The impact of raindrops on Salvinia molesta leaves: effects of trichomes and elasticity. J. R. Soc. Interface 18, 20210676. https://doi.org/10.1098/rsif.2021.0676.

Lauderbaugh, L.K., Ginebra-Solanellas, R.M., Holder, C.D., Webb, R., 2021. A biomechanical model of leaf inclination angle oscillations after raindrop impact. Environ. Exp. Bot. 190, 104586 https://doi.org/10.1016/j.envexpbot.2021.104586.

Laws, J.O., 1941. Measurements of the fall-velocity of water-drops and raindrops. Eos, Transactions American Geophysical Union 22, 709–721. https://doi.org/10.1029/TR022i003p00709.

Levia, D.F., Hudson, S.A., Llorens, P., Nanko, K., 2017. Throughfall drop size distributions: a review and prospectus for future research. WIREs Water 4, e1225. https://doi.org/10.1002/wat2.1225.

Levia, D.F., Nanko, K., Amasaki, H., Giambelluca, T.W., Hotta, N., Iida, S., Mudd, R.G., Nullet, M.A., Sakai, N., Shinohara, Y., Sun, X., Suzuki, M., Tanaka, N., Tantasirin, C., Yamada, K., 2019. Throughfall partitioning by trees. Hydrol. Process. 33, 1698–1708. https://doi.org/10.1002/hyp.13432.

Linhoss, A.C., Siegert, C.M., 2020. Calibration reveals limitations in modeling rainfall interception at the storm scale. J. Hydrol. 584, 124624 https://doi.org/10.1016/j.jhydrol.2020.124624.

Liu, S., 1997. A new model for the prediction of rainfall interception in forest canopies. Ecol. Model. 99, 151–159. https://doi.org/10.1016/S0304-3800(97)01948-0.

Lüpke, M., Leuchner, M., Levia, D., Nanko, K., Iida, S., Menzel, A., 2019. Characterization of differential throughfall drop size distributions beneath European beech and Norway spruce. Hydrol. Process. 33, 3391–3406. https://doi.org/10.1002/hyp.13565.

Marshall, J.S., Palmer, W.M.K., 1948. The distribution of raindrops with size. J. Atmos. Sci. 5, 165–166. https://doi.org/10.1175/1520-0469(1948)005<0165:TDORWS>2.0.CO;2.

Massman, W.J., 1980. Water storage on forest foliage: A general model. Water Resour. Res. 16, 210–216. https://doi.org/10.1029/WR016i001p00210.

Michalzik, B., Levia, D.F., Bischoff, S., Näthe, K., Richter, S., 2016. Effects of aphid infestation on the biogeochemistry of the water routed through European beech (Fagus sylvatica L.) saplings. Biogeochemistry 129, 197–214. https://doi.org/10.1007/s10533-016-0228-2.

Moss, A.J., Green, T.W., 1987. Erosive effects of the large water drops (gravity drops) that fall from plants. Soil Res. 25, 9–20. https://doi.org/10.1071/sr9870009.

Mulder, J.P.M., 1985. Simulating Interception Loss Using Standard Meteorological Data, in: Hutchison, B.A., Hicks, B.B. (Eds.), The Forest-Atmosphere Interaction: Proceedings of the Forest Environmental Measurements Conference Held at Oak Ridge, Tennessee, October 23–28, 1983. Springer Netherlands, Dordrecht, pp. 177–196. doi:10.1007/978-94-009-5305-5_12.

Nanko, K., Hotta, N., Suzuki, M., 2006. Evaluating the influence of canopy species and meteorological factors on throughfall drop size distribution. J. Hydrol. 329, 422–431. https://doi.org/10.1016/j.jhydrol.2006.02.036.

Nanko, K., Onda, Y., Ito, A., Moriwaki, H., 2008. Effect of canopy thickness and canopy saturation on the amount and kinetic energy of throughfall: An experimental approach. Geophys. Res. Lett. 35 https://doi.org/10.1029/2007GL033010.

Nanko, K., Onda, Y., Ito, A., Moriwaki, H., 2011. Spatial variability of throughfall under a single tree: Experimental study of rainfall amount, raindrops, and kinetic energy. Agric. For. Meteorol. 151, 1173–1182. https://doi.org/10.1016/j.agrformet.2011.04.006.

Nanko, K., Watanabe, A., Hotta, N., Suzuki, M., 2013. Physical interpretation of the difference in drop size distributions of leaf drips among tree species. Agric. For. Meteorol. 169, 74–84. https://doi.org/10.1016/j.agrformet.2012.09.018.

Nanko, K., Hudson, S.A., Levia, D.F., 2016. Differences in throughfall drop size distributions in the presence and absence of foliage. Hydrol. Sci. J. 61, 620–627. https://doi.org/10.1080/02626667.2015.1052454.

Nanko, K., Tanaka, N., Leuchner, M., Levia, D.F., 2020. Throughfall Erosivity in Relation to Drop Size and Crown Position: A Case Study from a Teak Plantation in Thailand. In: Levia, D.F., Carlyle-Moses, D.E., Iida, S., Michalzik, B., Nanko, K., Tischer, A. (Eds.), Forest-Water Interactions, Ecological Studies. Springer International Publishing, Cham, pp. 279–298. https://doi.org/10.1007/978-3-030-26086-6_12.

Pinos, J., Latron, J., Nanko, K., Levia, D.F., Llorens, P., 2020. Throughfall isotopic composition in relation to drop size at the intra-event scale in a Mediterranean Scots pine stand. Hydrol. Earth Syst. Sci. 24 https://doi.org/10.5194/hess-24-4675-2020.

Puckett, L.J., 1990. Estimates of ion sources in deciduous and coniferous throughfall. Atmos. Environ. Part A 24, 545–555. https://doi.org/10.1016/0960-1686(90)90009-C.

Raupach, M.R., Finnigan, J.J., 1988. "Single-Layer Models of Evaporation From Plant Canopies Are Incorrect but Useful, Whereas Multilayer Models Are Correct but Useless": Discuss. Functional Plant Biol. 15, 705–716. https://doi.org/10.1071/pp9880705.

Robson, A.J., Neal, C., Ryland, G.P.P., Harrow, M., 1994. Spatial variations in throughfall chemistry at the small plot scale. J. Hydrol. 158, 107–122. https://doi.org/10.1016/0022-1694(94)90048-5.

Roth-Nebelsick, A., Konrad, W., Ebner, M., Miranda, T., Thielen, S., Nebelsick, J.H., 2022. When rain collides with plants — patterns and forces of drop impact and how leaves respond to them. Journal of Experimental Botany erac004. https://doi.org/10.1093/jxb/erac004.

Rutter, A.J., Kershaw, K.A., Robins, P.C., Morton, A.J., 1971. A predictive model of rainfall interception in forests, 1. Derivation of the model from observations in a plantation of Corsican pine. Agric. Meteorol. 9, 367–384. https://doi.org/10.1016/0002-1571(71)90034-3.

Schymanski, S.J., Or, D., 2017. Leaf-scale experiments reveal an important omission in the Penman-Monteith equation. Hydrol. Earth Syst. Sci. 21, 685–706. https://doi.org/10.5194/hess-21-685-2017.

Tucker, A., Levia, D.F., Katul, G.G., Nanko, K., Rossi, L.F., 2020. A network model for stemflow solute transport. Appl. Math. Model. 88, 266–282. https://doi.org/10.1016/j.apm.2020.06.047.

Van Dijk, A.I.J.M., Gash, J.H., Van Gorsel, E., Blanken, P.D., Cescatti, A., Emmel, C., Gielen, B., Harman, I.N., Kiely, G., Merbold, L., Montagnani, L., Moors, E., Sottocornola, M., Varlagin, A., Williams, C.A., Wohlfahrt, G., 2015. Rainfall interception and the coupled surface water and energy balance. Agric. For. Meteorol. 214–215, 402–415. https://doi.org/10.1016/j.agrformet.2015.09.006.

Vrugt, J.A., Dekker, S.C., Bouten, W., 2003. Identification of rainfall interception model parameters from measurements of throughfall and forest canopy storage. Water Resour. Res. 39 https://doi.org/10.1029/2003WR002013.

Wang, P.K., Pruppacher, H.R., 1977. Acceleration to Terminal Velocity of Cloud and Raindrops. J. Appl. Meteorol. Climatology 16, 275–280. https://doi.org/10.1175/1520-0450(1977)016<0275:ATTVOC>2.0.CO;2.

Whelan, M.J., Sanger, L.J., Baker, M., Anderson, J.M., 1998. Spatial patterns of throughfall and mineral ion deposition in a lowland Norway spruce (Picea abies) plantation at the plot scale. Atmos. Environ. 32, 3493–3501. https://doi.org/10.1016/S1352-2310(98)00054-5.

Yarin, A.L., 2006. DROP IMPACT DYNAMICS: Splashing, Spreading, Receding, Bouncing…. Annu. Rev. Fluid Mech. 38, 159–192. https://doi.org/10.1146/annurev.fluid.38.050304.092144.

Zhang, Y., Wang, X., Pan, Y., Hu, R., 2021. How do rainfall intensity and raindrop size determine stemflow production? Quantitative evaluation from field rainfall simulation experiments. Hydrol. Sci. J. 66, 1979–1985. https://doi.org/10.1080/02626667.2021.1974024.

Zhu, Z., Zhu, D., Ge, M., 2021. The Spatial Variation Mechanism of Size, Velocity, and the Landing Angle of Throughfall Droplets under Maize Canopy. Water 13, 2083. https://doi.org/10.3390/w13152083.